

# Rate-Splitting for Multi-Antenna Non-Orthogonal Unicast and Multicast Transmission: Spectral and Energy Efficiency Analysis

Yijie Mao, *Student Member, IEEE*, Bruno Clerckx, *Senior Member, IEEE*, and Victor O.K. Li, *Fellow, IEEE*,

**Abstract**—In a non-orthogonal unicast and multicast transmission system, a multicast stream intended to all the users is superimposed in the power domain on the unicast streams. A conventional approach is based on Multi-User Linear Precoding (MU–LP) where each user relies on Successive Interference Cancellation (SIC) to first remove and decode the multicast stream before decoding its intended unicast stream. In this paper, we investigate the application of power-domain Non-Orthogonal Multiple Access (NOMA) and linearly-precoded Rate-Splitting (RS) in the non-orthogonal unicast and multicast transmission. Two different objectives are studied, namely maximizing the Weighted Sum Rate (WSR) and maximizing the Energy Efficiency (EE). Numerical results show that the proposed RS-assisted transmission strategy is more spectrally and energy efficient than the conventional MU–LP in a wide range of user deployments (with a diversity of channel directions, channel strengths and qualities of channel state information at the transmitter) and network loads (underloaded and overloaded regimes). Moreover, the WSR and EE performance gains of RS come without any increase in the receiver complexity compared with MU–LP. In comparison with the proposed NOMA-assisted transmission strategies, RS achieves better WSR and EE performance in a wide range of user deployments and network loads with much less complex receivers. Hence, we conclude that the proposed RS-assisted strategy is superior for downlink multi-antenna non-orthogonal unicast and multicast transmission.

**Index Terms**—non-orthogonal unicast and multicast transmission, rate-splitting, rate region, NOMA

## I. INTRODUCTION

Motivated by the scarcity of the radio resources in the Fifth Generation (5G) and beyond as well as the theory of Superposition Coding (SC), researchers have focused on the non-orthogonal unicast and multicast transmission [2]–[8] where the unicast and multicast services are enabled in the same time-frequency resource blocks. Such a transmission also finds applications as Layered Division Multiplexing (LDM) in the digital TV standard ATSC 3.0 [9]. LDM has been shown to achieve a higher spectral efficiency than Time Division Multiplexing (TDM)/Frequency Division Multiplexing (FDM) in [10]. From an information-theoretic perspective, SC combined with Dirty Paper Coding (DPC) is first investigated in [11] and further proved in [12] to achieve the capacity region of the two-user non-orthogonal unicast and multicast transmission systems.

This work is partially supported by the U.K. Engineering and Physical Sciences Research Council (EPSRC) under grant EP/N015312/1.

A preliminary version of this paper was presented at the 19th IEEE International workshop on Signal Processing advances in Wireless Communications (SPAWC) 2018 [1].

However, due to the high computational burden of implementing DPC, Multiuser Linear Precoding (MU–LP) becomes the most attractive alternative to simplify the transmitter design. At the transmitter, the multicast stream intended for all the users and the independent unicast streams are linearly precoded and superimposed before sending to the users. At each user, the multicast stream is first decoded and removed using Successive Interference Cancellation (SIC) and then the intended unicast stream is decoded by fully treating any residual interference as noise. Such MU–LP-assisted transmission has been studied previously with the objective of minimizing the transmit power [5], [6], maximizing the Weighted Sum Rate (WSR) [7] or the Energy Efficiency (EE) [8]. The benefit of MU–LP-assisted transmission is to exploit all spatial multiplexing gains of a multi-antenna Broadcast Channel (BC) with perfect Channel State Information at the Transmitter (CSIT). However, MU–LP is mainly suited to the underloaded regime (where the number of users is smaller than the number of transmit antennas). It is sensitive to the user channel orthogonality and strengths, and does not optimally exploit the multiplexing gain of a multi-antenna BC with imperfect CSIT [13]. Moreover, the presence of SIC at the receivers is not exploited to manage the interference among the unicast streams, but only to separate the multicast stream from the unicast streams. In this paper, we try to resolve the above limitations of MU–LP by resorting to two different approaches, namely, power-domain Non-Orthogonal Multiple Access (NOMA) and Rate-Splitting (RS).

Power-domain NOMA (referred to simply as NOMA in the rest of the paper) relies on SC at the transmitter and SIC at the receivers (SC–SIC) [14]. It forces some users to fully decode and cancel the interference created by other users. Recent attentions have been paid to the application of NOMA in the non-orthogonal unicast and multicast transmission [15]–[17]. However, these works do not consider the same non-orthogonal unicast and multicast transmission system as in the previous MU–LP-assisted transmission. In [15], [17], the term NOMA is used to represent the non-orthogonal unicast and multicast transmission where the Base Station (BS) transmits a single unicast stream for one user together with a multicast stream for all the users. The SIC is used to separate the unicast and the multicast streams. This is a simpler transmission scheme comparing with MU–LP. In [16], the users requiring the unicast streams are separated from the users requiring the multicast stream. The users requiring the multicast stream decode all the multicast and unicast streams based on SIC and serve as

relays for other users. The benefits of using SIC in NOMA-assisted non-orthogonal unicast and multicast transmissions have not been fully exploited yet. Comparing with MU-LP, the advantage of NOMA is to cope with an overloaded regime where multiple users experience different channel strengths. However, NOMA is inefficient to exploit the spatial dimensions in general multi-antenna settings with both perfect and imperfect CSIT (leading to a multiplexing gain loss). It is motivated by specific user deployments (aligned channels with channel strength disparities) and is subject to a significant complexity increase at the transmitter (user grouping, user ordering) and the receivers (multiple layers of SIC) [13].

In contrast with MU-LP that relies on fully treating interference as noise and NOMA that relies on some users to fully decode interference, linearly-precoded RS, introduced as a multi-user multi-antenna non-orthogonal transmission strategy in [18], enables one to partially decode the interference and partially treat the interference as noise. This allows RS to explore a more general and powerful transmission framework for downlink multi-antenna systems that contains MU-LP and NOMA as special cases, and provides room for rate and Quality of Service (QoS) enhancements and complexity reduction [13]. RS has been investigated in the unicast-only transmission with perfect CSIT [13], [19]–[21] and imperfect CSIT [22]–[24]. Each unicast stream is split at the transmitter into a common part and a private part. The common parts are jointly encoded into one common stream to be decoded by all the users while the private parts are independently encoded into the private streams to be decoded by the intended users. Due to the superimposed transmission of the common and private streams, RS can be viewed mathematically as a non-orthogonal unicast and multicast transmission. Hence, RS was termed joint multicasting and broadcasting in [25]. Though both the common stream in the RS-assisted unicast-only transmission and the conventional multicast stream are decoded by all the users, they are transmitted with different intentions. The multicast stream is intended for all users while the common stream in RS is intended for part of the users.

Motivated by the benefits of RS in the unicast-only transmission, we study the application of RS in the non-orthogonal unicast and multicast transmission in this paper. The contributions of the paper are summarized as follows:

- We propose a RS-assisted non-orthogonal unicast and multicast transmission strategy and design the precoder to maximize WSR and EE, respectively. By splitting the unicast streams into common and private parts and encoding the common parts along with the multicast stream into a super-common stream to be decoded by all users, the SIC in RS is used for the dual purpose of separating the unicast and multicast streams as well as managing the interference among the unicast streams.
- We propose two NOMA-assisted non-orthogonal unicast and multicast transmission strategies, namely, 'SC-SIC' and 'SC-SIC per group'. Both the WSR and EE maximization problems subject to the QoS rate requirements and a sum power constraint are investigated for each proposed transmission strategy.

- We propose two optimization frameworks to solve the WSR and EE maximization problems based on the Weighted Minimum Mean Square Error (WMMSE) and Successive Convex Approximation (SCA) algorithms, respectively. The effectiveness of the proposed algorithms is verified in the numerical results.
- We show through numerical results that the proposed RS-assisted transmission strategy is more spectrally and energy efficient than the existing MU-LP-assisted transmission in a wide range of user deployments (with a diversity of channel directions, channel strengths and qualities of channel state information at the transmitter) and network loads (underloaded and overloaded regimes). Importantly, applying RS to the non-orthogonal unicast and multicast transmission boosts WSR and EE of the system but maintains the same receiver complexity as MU-LP. RS makes a better use of the existing one layer of SIC. Comparing with the proposed NOMA-assisted transmission strategies, RS achieves a more robust WSR and EE performance in a wide range of user deployments and network loads while its receiver complexity is much lower than the NOMA-assisted transmission strategies.

The rest of the paper is organized as follows. Section II introduces the system and power model. Section III reviews the existing MU-LP strategy. Section IV and V specify the proposed NOMA and RS strategies, respectively. Section VI discusses the optimization frameworks to solve the WSR and EE problems. Section VII and VIII illustrate numerical results of WSR and EE. Section IX concludes the paper.

## II. SYSTEM MODEL AND POWER MODEL

### A. System Model

Consider a BS equipped with  $N_t$  antennas serving  $K$  single-antenna users in the user group  $\mathcal{K} = \{1, \dots, K\}$ . In each time frame, user- $k$ ,  $k \in \mathcal{K}$  requires a dedicated unicast message  $W_k$  and a multicast message  $W_0$ . At the BS, the multicast message  $W_0$  intended for all the users and the  $K$  unicast messages  $W_1, \dots, W_K$  are encoded into the  $(K + 1)$  dimensional data stream vector  $\mathbf{s}$  and linearly precoded using the precoder  $\mathbf{P}$ . The transmit signal vector is  $\mathbf{x} = \mathbf{Ps}$ . It is subject to the power constraint  $\mathbb{E}\{\|\mathbf{x}\|^2\} \leq P_t$ . Assuming that  $\mathbb{E}\{\mathbf{ss}^H\} = \mathbf{I}$ , we have  $\text{tr}(\mathbf{PP}^H) \leq P_t$ . The signal received at user- $k$  is  $y_k = \mathbf{h}_k^H \mathbf{x} + n_k, \forall k \in \mathcal{K}$ , where  $\mathbf{h}_k \in \mathbb{C}^{N_t \times 1}$  is the channel between the BS and user- $k$ , it is assumed to be perfectly known at the transmitter and receivers. The imperfect CSIT scenario will be discussed in the proposed algorithm and numerical results. The received noise  $n_k$  is modeled as a complex Gaussian random variable with zero mean and variance  $\sigma_{n,k}^2$ . Without loss of generality, we assume the noise variances are equal to one ( $\sigma_{n,k}^2 = 1, \forall k \in \mathcal{K}$ ). The transmit Signal-to-Noise Ratio (SNR) is equal to the total power consumption  $P_t$ .

### B. Power Consumption Model

In this work, the total power consumption at the BS is [26]

$$P_{\text{total}} = \frac{1}{\eta} \text{tr}(\mathbf{PP}^H) + P_{\text{cir}}, \quad (1)$$

where  $\eta \in [0, 1]$  is the power amplifier efficiency.  $P_{\text{cir}} = N_t P_{\text{dyn}} + P_{\text{sta}}$  is the circuit power consumption of the BS,

where  $P_{\text{dyn}}$  is the dynamic power consumption of one active radio frequency chain and  $P_{\text{sta}}$  is the static power consumption of the cooling systems, power supply and so on.  $\eta$  and  $P_{\text{sta}}$  are assumed to be fixed for simplicity.

### III. EXISTING MU-LP-ASSISTED TRANSMISSION

In the existing MU-LP-assisted transmission, the multicast and unicast messages  $W_0, W_1, \dots, W_K$  are independently encoded into the data streams  $s_0, s_1, \dots, s_K$ . The stream vector  $\mathbf{s} = [s_0, s_1, \dots, s_K]^T$  is precoded using the precoder  $\mathbf{P} = [\mathbf{p}_0, \mathbf{p}_1, \dots, \mathbf{p}_K]$ , where  $\mathbf{p}_0, \mathbf{p}_k \in \mathbb{C}^{N_t \times 1}$  are the respective precoders of the multicast stream  $s_0$  and the unicast stream  $s_k$ . The resulting transmit signal  $\mathbf{x} \in \mathbb{C}^{N_t \times 1}$  is given by

$$\mathbf{x} = \mathbf{Ps} = \underbrace{\mathbf{p}_0 s_0}_{\text{multicast stream}} + \underbrace{\sum_{k \in \mathcal{K}} \mathbf{p}_k s_k}_{\text{unicast streams}}. \quad (2)$$

The signal received at user- $k$  becomes

$$\begin{aligned} y_k = & \underbrace{\mathbf{h}_k^H \mathbf{p}_0 s_0}_{\text{intended multicast stream}} + \underbrace{\mathbf{h}_k^H \mathbf{p}_k s_k}_{\text{intended unicast stream}} \\ & + \underbrace{\sum_{j \in \mathcal{K}, j \neq k} \mathbf{h}_k^H \mathbf{p}_j s_j}_{\text{interference among unicast streams}} + n_k. \end{aligned} \quad (3)$$

Each user first decodes the multicast stream  $s_0$  by treating the signal of the unicast streams as interference. The Signal-to-Interference-plus-Noise Ratio (SINR) of  $s_0$  at user- $k$  is

$$\gamma_{k,0} = \frac{|\mathbf{h}_k^H \mathbf{p}_0|^2}{\sum_{j \in \mathcal{K}} |\mathbf{h}_k^H \mathbf{p}_j|^2 + 1}. \quad (4)$$

Once  $s_0$  is successfully decoded and subtracted from the original received signal  $y_k$ , user- $k$  decodes the intended unicast stream  $s_k$  by treating the interference of the unicast streams of other users as noise. The SINR of decoding  $s_k$  at user- $k$  is

$$\gamma_k = \frac{|\mathbf{h}_k^H \mathbf{p}_k|^2}{\sum_{j \in \mathcal{K}, j \neq k} |\mathbf{h}_k^H \mathbf{p}_j|^2 + 1}. \quad (5)$$

The corresponding achievable rates of  $s_0$  and  $s_k$  at user- $k$  are

$$R_{k,0} = \log_2 (1 + \gamma_{k,0}), R_k = \log_2 (1 + \gamma_k). \quad (6)$$

To ensure that  $s_0$  is successfully decoded by all users, the achievable rate of  $s_0$  shall not exceed

$$R_0 = \min \{R_{1,0}, \dots, R_{K,0}\}. \quad (7)$$

1) *Weighted sum rate maximization problem:* To investigate the spectral efficiency, we study the problem of maximizing the WSR of the unicast messages while the QoS rate constraints of all the streams and the power constraint of the BS should be met. For a given weight vector  $\mathbf{u} = [u_1, \dots, u_K]$ , the WSR maximization problem in the  $K$ -user MU-LP-assisted non-orthogonal unicast and multicast transmission is

$$\begin{aligned} \text{WSR}_{\text{MU-LP}} = & \max_{\mathbf{P}} \sum_{k \in \mathcal{K}} u_k R_k \quad (8a) \\ \text{s.t.} \quad & R_k \geq R_k^{th}, \forall k \in \mathcal{K} \quad (8b) \\ & R_{k,0} \geq R_0^{th}, \forall k \in \mathcal{K} \quad (8c) \\ & \text{tr}(\mathbf{P} \mathbf{P}^H) \leq P_t \quad (8d) \end{aligned}$$

where constraint (8b) is the QoS rate requirement of each unicast stream.  $R_k^{th}$  is the rate lower bound of the unicast stream  $s_k$ . Constraint (8c) ensures that each user decodes the multicast stream  $s_0$  with a rate larger than or equal to  $R_0^{th}$ .

2) *Energy efficiency maximization problem:* To investigate the EE of MU-LP, we maximize the WSR of all the streams divided by the sum power of the transmitter. For a given weight vector  $\mathbf{u}_{\text{tot}} = [u_0, u_1, \dots, u_K]$  of all the streams, the EE maximization problem of MU-LP is

$$\begin{aligned} \text{EE}_{\text{MU-LP}} = & \max_{\mathbf{P}} \frac{u_0 R_0 + \sum_{k \in \mathcal{K}} u_k R_k}{\frac{1}{\eta} \text{tr}(\mathbf{P} \mathbf{P}^H) + P_{\text{cir}}} \quad (9) \\ \text{s.t.} \quad & (8b), (8c), (8d) \end{aligned}$$

MU-LP does not require any SIC at each user in the unicast-only transmission. In comparison, one layer of SIC is necessary at each user to remove the multicast stream before decoding the intended unicast stream in the MU-LP-assisted non-orthogonal unicast and multicast transmission. The SIC is used for the purpose of separating the unicast and multicast streams.

### IV. PROPOSED NOMA-ASSISTED TRANSMISSION

There are two main strategies in the multi-antenna NOMA, namely, 'SC-SIC' and 'SC-SIC per group' [13]. Both strategies are applied in the non-orthogonal unicast and multicast transmission and explained in this section. Comparing with the existing MU-LP, NOMA-assisted transmissions require more layers of SIC at each user to decode the interference.

#### A. SC-SIC

In the SC-SIC-assisted non-orthogonal unicast and multicast transmission, the interference among the unicast streams is cancelled by allowing users to decode the unicast streams of other co-channel users successively based on certain decoding order until the intended stream is decoded. The decoding order  $\pi$  of the unicast stream is required to be optimized together with the precoder. For a given  $\pi$ , we assume the unicast message  $W_{\pi(k)}$  is decoded before the unicast message  $W_{\pi(j)}$ ,  $\forall k \leq j$ . Therefore, the unicast message  $W_{\pi(1)}$  of user- $\pi(1)$  is decoded by all the users while the unicast message  $W_{\pi(K)}$  of user- $\pi(K)$  is decoded by user- $\pi(K)$  only. As both the multicast message  $W_0$  and the unicast message  $W_{\pi(1)}$  are required to be decoded by all the users, they are jointly encoded into one stream  $s_{0,\pi(1)}$ . The messages  $W_{\pi(2)}, \dots, W_{\pi(K)}$  are independently encoded into the streams  $s_{\pi(2)}, \dots, s_{\pi(K)}$ . The formed stream vector  $\mathbf{s} = [s_{0,\pi(1)}, s_{\pi(2)}, \dots, s_{\pi(K)}]^T$  is precoded by  $\mathbf{P} = [\mathbf{p}_{0,\pi(1)}, \mathbf{p}_{\pi(2)}, \dots, \mathbf{p}_{\pi(K)}]$ . The transmit signal becomes

$$\mathbf{x} = \mathbf{Ps} = \underbrace{\mathbf{p}_{0,\pi(1)} s_{0,\pi(1)}}_{\text{multicast stream and the unicast stream of user-}\pi(1)} + \underbrace{\sum_{k > 1, k \in \mathcal{K}} \mathbf{p}_{\pi(k)} s_{\pi(k)}}_{\text{unicast streams}}. \quad (10)$$

At user sides, each user first decode  $s_{0,\pi(1)}$ . The SINR at user- $\pi(k)$  to decode the  $s_{0,\pi(1)}$  is

$$\gamma_{\pi(k) \rightarrow (0,\pi(1))} = \frac{|\mathbf{h}_{\pi(k)}^H \mathbf{p}_{0,\pi(1)}|^2}{\sum_{j > 1, j \in \mathcal{K}} |\mathbf{h}_{\pi(k)}^H \mathbf{p}_{\pi(j)}|^2 + 1}. \quad (11)$$

As  $s_{0,\pi(1)}$  is decoded by all the users, the rate of  $s_{0,\pi(1)}$  shall not exceed  $R_{0,\pi(1)} = \min_{k \in \mathcal{K}} \{\log_2 (1 + \gamma_{\pi(k) \rightarrow (0,\pi(1))})\}$ . Note that  $R_{0,\pi(1)}$  is shared by the rates of the multicast stream and the unicast stream of user- $\pi(1)$  denoted by  $C_0$  and  $C_{\pi(1)}$ , respectively. We have  $R_{0,\pi(1)} = C_0 + C_{\pi(1)}$ .

At user- $\pi(1)$ , the intended unicast message and the multicast message are encapsulated in  $s_{0,\pi(1)}$ . By decoding  $s_{0,\pi(1)}$ , user- $\pi(1)$  directly decodes the intended  $W_0$  and  $W_{\pi(1)}$  since they are

encapsulated in  $s_{0,\pi(1)}$ . All other users carry on decoding the unicast messages based on the decoding order  $\pi$  after decoding  $s_{0,\pi(1)}$ . The SINR experienced at user- $\pi(i)$ ,  $i > 1$  to decode the unicast message of user- $\pi(k)$ ,  $1 < k \leq i$  is

$$\gamma_{\pi(i) \rightarrow \pi(k)} = \frac{|\mathbf{h}_{\pi(i)}^H \mathbf{p}_{\pi(k)}|^2}{\sum_{j>k, j \in \mathcal{K}} |\mathbf{h}_{\pi(i)}^H \mathbf{p}_{\pi(j)}|^2 + 1}. \quad (12)$$

The unicast stream  $s_{\pi(k)}$  intended for user- $\pi(k)$  is decoded by user- $\pi(i)$ ,  $\forall i \geq k, i \in \mathcal{K}$ . To ensure  $s_{\pi(k)}$  is successfully decoded by the users, the achievable rate of  $s_{\pi(k)}$  is  $R_{\pi(k)} = \min_{i \geq k, i \in \mathcal{K}} \{\log_2 (1 + \gamma_{\pi(i) \rightarrow \pi(k)})\}$ .

1) *Weighted sum rate maximization problem*: Following the WSR maximization problem of MU-LP, the WSR maximization problem in the  $K$ -user SC-SIC-assisted non-orthogonal unicast and multicast transmission for a given  $\mathbf{u}$  is

$$\left. \begin{array}{l} \max_{\pi, \mathbf{P}, \mathbf{c}} u_{\pi(1)} C_{\pi(1)} + \sum_{k>1, k \in \mathcal{K}} u_{\pi(k)} R_{\pi(k)} \\ \text{s.t. } R_{\pi(k)} \geq R_{\pi(k)}^{th}, \forall k \in \{2, \dots, K\} \\ C_{\pi(1)} \geq R_{\pi(1)}^{th} \\ C_0 \geq R_0^{th} \\ C_0 + C_{\pi(1)} \leq R_{0,\pi(1)} \\ \text{tr}(\mathbf{P} \mathbf{P}^H) \leq P_t \end{array} \right\} \begin{array}{l} (13a) \\ (13b) \\ (13c) \\ (13d) \\ (13e) \\ (13f) \end{array}$$

where  $\mathbf{c} = [C_0, C_{\pi(1)}]$  is the rate vector containing the portions of the rate allocated to  $W_0$  and  $W_{\pi(1)}$ , respectively.  $\mathbf{c}$  is required to be maximized with the decoding order  $\pi$  and the precoder  $\mathbf{P}$  so as to maximize the WSR. Constraints (13b)–(13d) are the QoS rate constraints. Constraint (13e) ensures that  $s_{0,\pi(1)}$  is successfully decoded by all the users.

2) *Energy efficiency maximization problem*: For a given  $\mathbf{u}_{tot}$ , the EE maximization problem of SC-SIC is given by

$$\left. \begin{array}{l} \max_{\pi, \mathbf{P}, \mathbf{c}} \frac{u_0 C_0 + u_{\pi(1)} C_{\pi(1)} + \sum_{k>1, k \in \mathcal{K}} u_{\pi(k)} R_{\pi(k)}}{\frac{1}{\eta} \text{tr}(\mathbf{P} \mathbf{P}^H) + P_{cir}} \\ \text{s.t. } (13b), (13c), (13d), (13e), (13f) \end{array} \right\} \quad (14)$$

Similarly to the  $K$ -user SC-SIC-assisted unicast-only transmission,  $K - 1$  layers of SIC is required at each user in the  $K$ -user non-orthogonal unicast and multicast transmission. But the first layer of SIC is used for different purposes. It is used not only to decode the multi-user interference among the unicast streams, but also to separate the unicast and multicast streams.

### B. SC-SIC per group

In the unicast-only transmission, SC-SIC per group can be regarded as a more general strategy than SC-SIC [13]. It consists of grouping  $K$  users into  $G$  separated groups. Users within each group are served using SC-SIC and users across the groups are served using MU-LP [13]. SC-SIC is the special case when there is only one group of users ( $G = 1$ ). In contrast with the unicast-only transmission, the receiver complexity of SC-SIC per group increases in the non-orthogonal unicast and multicast transmission. As the inter-group interference is mitigated using MU-LP, none of the unicast messages can be encoded with the multicast message  $W_0$ . One more layer of SIC is required to separate the multicast and unicast streams in the SC-SIC per group-assisted non-orthogonal unicast and multicast transmission.

We assume the  $K$  users are divided into  $G$  groups, denoted as  $\mathcal{G} = \{1, \dots, G\}$ . Each group- $g$ ,  $g \in \mathcal{G}$  contains a subset of users  $\mathcal{K}_g$ , where  $\mathcal{K}_g \subseteq \mathcal{K}$ . The user groups are separated and satisfy  $\cup_{g \in \mathcal{G}} \mathcal{K}_g = \mathcal{K}$  and  $\mathcal{K}_g \cap \mathcal{K}_{g'} = \emptyset$ , if  $g \neq g'$ . For a certain decoding order  $\pi_g$  for the users in group- $g$ , we assume the unicast message  $W_{\pi_g(k)}$  is decoded before the unicast message  $W_{\pi_g(j)}$ ,  $\forall k \leq j$ . The multicast and unicast messages are independently encoded and transmitted based on SC. The resulting transmit signal is the same as Equation (2).

At user sides, each user first decodes the multicast stream  $s_0$  by treating the signal of all the unicast streams as interference. The achievable rate of the multicast stream  $R_0$  is calculated by (6) and (7). Once  $s_0$  is decoded and removed using SIC, each user decodes the unicast streams based on the group-specific decoding order  $\pi_g$ ,  $g \in \mathcal{G}$ . User- $\pi_g(i)$  will decode  $s_{\pi_g(k)}$ ,  $\forall k \leq i$ . The SINR at user- $\pi_g(i)$  to decode  $s_{\pi_g(k)}$ ,  $k \leq i$  is [13]

$$\gamma_{\pi_g(i) \rightarrow \pi_g(k)} = \frac{|\mathbf{h}_{\pi_g(i)}^H \mathbf{p}_{\pi_g(k)}|^2}{\sum_{j>k, j \in \mathcal{K}_g} |\mathbf{h}_{\pi_g(i)}^H \mathbf{p}_{\pi_g(j)}|^2 + I_{\pi_g(i)} + 1}, \quad (15)$$

where  $I_{\pi_g(i)} = \sum_{g' \in \mathcal{G}, g' \neq g} \sum_{j \in \mathcal{K}_{g'}} |\mathbf{h}_{\pi_g(i)}^H \mathbf{p}_j|^2$  is the inter-group interference suffered by user- $\pi_g(i)$ . The achievable rate of  $s_{\pi_g(k)}$  is  $R_{\pi_g(k)} = \min_{i \geq k, i \in \mathcal{K}_g} \{\log_2 (1 + \gamma_{\pi_g(i) \rightarrow \pi_g(k)})\}$ .

1) *Weighted sum rate maximization problem*: The WSR problem in the  $K$ -user SC-SIC per group-assisted non-orthogonal unicast and multicast transmission for a given  $\mathbf{u}$  is

$$\left. \begin{array}{l} \max_{\pi, \mathbf{P}, \mathbf{c}} \sum_{\{K_g\}, \mathcal{G}} \sum_{g \in \mathcal{G}} \sum_{k \in \mathcal{K}_g} u_{\pi_g(k)} R_{\pi_g(k)} \\ \text{s.t. } R_{\pi_g(k)} \geq R_{\pi_g(k)}^{th}, \forall k \in \mathcal{K}_g, g \in \mathcal{G} \\ R_{k,0} \geq R_0^{th}, \forall k \in \mathcal{K} \\ \text{tr}(\mathbf{P} \mathbf{P}^H) \leq P_t \end{array} \right\} \begin{array}{l} (16a) \\ (16b) \\ (16c) \\ (16d) \end{array}$$

The user ordering  $\pi = \{\pi_1, \dots, \pi_G\}$  and user grouping  $\{\mathcal{K}_g\}, \mathcal{G}$  are required to be optimized with the precoder.

2) *Energy efficiency maximization problem*: The EE maximization problem of SC-SIC per group for a given  $\mathbf{u}_{tot}$  is

$$\left. \begin{array}{l} \max_{\pi, \mathbf{P}, \mathbf{c}} \frac{u_0 R_0 + \sum_{g \in \mathcal{G}} \sum_{k \in \mathcal{K}_g} u_{\pi_g(k)} R_{\pi_g(k)}}{\frac{1}{\eta} \text{tr}(\mathbf{P} \mathbf{P}^H) + P_{cir}} \\ \text{s.t. } (16b), (16c), (16d) \end{array} \right\} \quad (17)$$

Different from the SC-SIC per group-assisted unicast-only transmission where  $|\mathcal{K}_g| - 1$  layers of SIC are required at each user within the user group  $\mathcal{K}_g$ ,  $\forall g \in \mathcal{G}$  to decode the inner-group interference,  $|\mathcal{K}_g|$  layers of SIC are required at each user in the SC-SIC per group-assisted non-orthogonal unicast and multicast transmission. The one additional layer of SIC is introduced to separate the unicast and multicast streams.

## V. PROPOSED RATE-SPLITTING-ASSISTED TRANSMISSION

The  $K$ -user (1-layer) RS-assisted non-orthogonal unicast and multicast transmission model is illustrated in Fig. 1. The unicast message  $W_k$  intended for user- $k$ ,  $\forall k \in \mathcal{K}$  is split into a common part  $W_{k,c}$  and a private part  $W_{k,p}$ . The private parts of the unicast messages  $W_{1,p}, \dots, W_{K,p}$  are independently encoded into the private streams  $s_1, \dots, s_K$  while the common parts of the unicast messages  $W_{1,c}, \dots, W_{K,c}$  are jointly

encoded with the multicast message  $W_0$  into a super-common stream  $s_0$  required to be decoded by all users.  $s_0$  includes the whole multicast message as well as parts of the unicast messages. The formed stream vector  $\mathbf{s} = [s_0, s_1, \dots, s_K]^T$  is linearly precoded using the precoder  $\mathbf{P} = [\mathbf{p}_0, \mathbf{p}_1, \dots, \mathbf{p}_K]$ . The resulting transmit signal  $\mathbf{x} \in \mathbb{C}^{N_t \times 1}$  is

$$\mathbf{x} = \underbrace{\mathbf{p}_0 s_0}_{\text{super-common stream}} + \sum_{k \in \mathcal{K}} \underbrace{\mathbf{p}_k s_k}_{\text{private streams}}. \quad (18)$$

The signal received at user- $k$  is

$$\begin{aligned} y_k = & \underbrace{\mathbf{h}_k^H \mathbf{p}_0 s_0}_{\text{super-common stream}} + \underbrace{\mathbf{h}_k^H \mathbf{p}_k s_k}_{\text{intended private stream}} \\ & + \underbrace{\sum_{j \in \mathcal{K}, j \neq k} \mathbf{h}_k^H \mathbf{p}_j s_j}_{\text{interference from co-scheduled private streams}} + n_k. \end{aligned} \quad (19)$$

The super-common stream and private streams are decoded using one layer of SIC in a similar way as decoding the multicast stream and the unicast streams in the MU-LP-assisted transmission strategy. Hence, the resulting achievable rate of the super-common stream  $R_{k,0}$  and the private stream  $R_k, \forall k \in \mathcal{K}$  are calculated by (6) and the achievable rate of the super-common stream  $R_0$  is calculated by (7). Since  $R_0$  is shared by the achievable rates of transmitting the multicast message  $W_0$  and the common parts of the unicast messages  $W_{1,c}, \dots, W_{K,c}$ , it is equal to  $C_0 + \sum_{k \in \mathcal{K}} C_{k,0} = R_0$ , where  $C_0$  is the portion of  $R_0$  transmitting  $W_0$  and  $C_{k,0}$  is the user- $k$ 's portion of  $R_0$  transmitting  $W_{k,c}$ . The total achievable rate of the unicast message of user- $k$  is  $R_{k,tot} = C_{k,0} + R_k$ .

1) *Weighted sum rate maximization problem:* The WSR maximization problem in the  $K$ -user RS-assisted non-orthogonal unicast and multicast transmission for a given  $\mathbf{u}$  is

$$\left\{ \begin{array}{l} \max_{\mathbf{P}, \mathbf{c}} \sum_{k \in \mathcal{K}} u_k R_{k,tot} \\ \text{s.t.} \quad C_{k,0} + R_k \geq R_k^{th}, \forall k \in \mathcal{K} \\ C_0 \geq R_0^{th} \\ C_0 + \sum_{k \in \mathcal{K}} C_{k,0} \leq R_{k,0}, \forall k \in \mathcal{K} \\ C_{k,0} \geq 0, \forall k \in \mathcal{K} \\ \text{tr}(\mathbf{P} \mathbf{P}^H) \leq P_t \end{array} \right. \quad \begin{array}{l} (20a) \\ (20b) \\ (20c) \\ (20d) \\ (20e) \\ (20f) \end{array}$$

where  $\mathbf{c} = [C_0, C_{1,0}, \dots, C_{K,0}]$  is the common rate vector required to be optimized with the precoder  $\mathbf{P}$ . When  $C_{k,0} = 0, \forall k \in \mathcal{K}$ , problem (20) reduces to problem (8). Hence, the proposed RS model always achieves the same or superior performance to MU-LP. Constraint (20d) ensures the super-common stream can be successfully decoded by all the users. Constraints (20b) and (20c) are the QoS rate constraints.

1) *Energy efficiency maximization problem:* The EE maximization problem of RS for a given  $\mathbf{u}_{tot}$  is

$$\left\{ \begin{array}{l} \max_{\mathbf{c}, \mathbf{P}} \frac{u_0 C_0 + \sum_{k \in \mathcal{K}} u_k R_{k,tot}}{\frac{1}{\eta} \text{tr}(\mathbf{P} \mathbf{P}^H) + P_{cir}} \\ \text{s.t.} \quad (20b), (20c), (20d), (20e), (20f) \end{array} \right. \quad (21)$$

Without the introduced multicast stream, the RS model explained above is similar to the '1-layer RS' discussed in

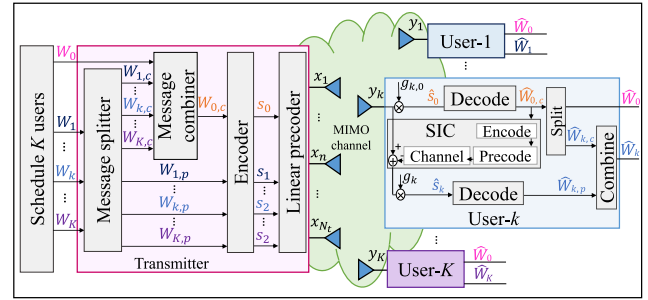


Fig. 1:  $K$ -user (1-layer) RS assisted multi-antenna non-orthogonal unicast and multicast transmission model

[13]. A more generalized RS-assisted unicast-only transmission model is proposed in [13] where the number of layers of the common streams is increasing with the number of serving users. It is a more general multiple access scheme than MU-LP, SC-SIC and SC-SIC per group. Only when  $K = 2$  will the generalized RS reduce to 1-layer RS.

Similarly to the  $K$ -user 1-layer RS-assisted unicast-only transmission, one layer of SIC is required at each user in the  $K$ -user (1-layer) RS-assisted non-orthogonal unicast and multicast transmission. Combining the benefit of the SIC used in the RS-assisted unicast-only transmission and in the MU-LP-assisted non-orthogonal unicast and multicast transmission, the SIC of RS-assisted non-orthogonal unicast and multicast transmission is used for separating the unicast and multicast streams as well as better managing the multi-user interference among the unicast streams. The presence of SIC is better exploited. Comparing with the proposed NOMA strategies, the receiver complexity of RS does not depend on the number of served users  $K$  and is much lower especially when  $K$  is large.

## VI. OPTIMIZATION FRAMEWORKS

In this section, we specify the optimization frameworks proposed to solve the WSR and EE maximization problems.

### A. WMMSE-based AO algorithm for WSR problems

The WMMSE algorithm to solve the sum rate maximization problem in RS without a multicast message is proposed in [23]. It is extended to solve the WSR maximization problems with QoS rate constraints of all the streams. We firstly explain the procedure to solve the RS problem (20) and then specify how (8), (13) and (16) can be solved correspondingly.

User- $k$  decodes the super-common stream  $s_0$  and the private stream  $s_k$  sequentially using one layer of SIC.  $s_0$  and  $s_k$  are respectively estimated using the equalizers  $g_{k,0}$  and  $g_k$ . Once  $s_0$  is successfully decoded by  $\hat{s}_0 = g_{k,0} y_k$  and removed from  $y_k$ ,  $s_k$  is decoded by  $\hat{s}_k = g_k(y_k - \mathbf{h}_k^H \mathbf{p}_0 \hat{s}_0)$ . The Mean Square Errors (MSEs) of decoding  $s_0$  and  $s_k$  are calculated as

$$\begin{aligned} \varepsilon_{k,0} &\triangleq \mathbb{E}\{|\hat{s}_{k,0} - s_{k,0}|^2\} = |g_{k,0}|^2 T_{k,0} - 2\Re\{g_{k,0} \mathbf{h}_k^H \mathbf{p}_0\} + 1, \\ \varepsilon_k &\triangleq \mathbb{E}\{|\hat{s}_k - s_k|^2\} = |g_k|^2 T_k - 2\Re\{g_k \mathbf{h}_k^H \mathbf{p}_k\} + 1, \end{aligned} \quad (22)$$

where  $T_{k,0} \triangleq |\mathbf{h}_k^H \mathbf{p}_0|^2 + \sum_{j \in \mathcal{K}} |\mathbf{h}_k^H \mathbf{p}_j|^2 + 1$  and  $T_k \triangleq T_{k,0} - |\mathbf{h}_k^H \mathbf{p}_0|^2$ . By solving  $\frac{\partial \varepsilon_{k,0}}{\partial g_{k,0}} = 0$  and  $\frac{\partial \varepsilon_k}{\partial g_k} = 0$ , the optimum MMSE equalizers are given by

$$g_{k,0}^{\text{MMSE}} = \mathbf{p}_0^H \mathbf{h}_k T_{k,0}^{-1}, \quad g_k^{\text{MMSE}} = \mathbf{p}_k^H \mathbf{h}_k T_k^{-1}. \quad (23)$$

Substituting (23) into (22), the MMSEs become  $\varepsilon_{k,0}^{\text{MMSE}} = (T_{k,0} - |\mathbf{h}_k^H \mathbf{p}_k|^2)/T_{k,0}$  and  $\varepsilon_k^{\text{MMSE}} = (T_k - |\mathbf{h}_k^H \mathbf{p}_k|^2)/T_k$ . Then the SINRs of  $s_0$  and  $s_k$  can be transformed to  $\gamma_{k,0} = 1/\varepsilon_{k,0}^{\text{MMSE}} - 1$  and  $\gamma_k = 1/\varepsilon_k^{\text{MMSE}} - 1$ . The rates become  $R_{k,0} = -\log_2(\varepsilon_{k,0}^{\text{MMSE}})$  and  $R_k = -\log_2(\varepsilon_k^{\text{MMSE}})$ .

By introducing the positive weights  $(w_{k,0}, w_k)$ , the WMSEs of decoding  $s_0$  and  $s_k$  at user- $k$  are defined as

$$\xi_{k,0} \triangleq w_{k,0}\varepsilon_{k,0} - \log_2(w_{k,0}), \quad \xi_k \triangleq w_k\varepsilon_k - \log_2(w_k). \quad (24)$$

Then the Rate-WMMSE relationships are established as

$$\begin{aligned} \xi_{k,0}^{\text{MMSE}} &\triangleq \min_{w_{k,0}, g_{k,0}} \xi_{k,0} = 1 - R_{k,0}, \\ \xi_k^{\text{MMSE}} &\triangleq \min_{w_k, g_k} \xi_k = 1 - R_k. \end{aligned} \quad (25)$$

where  $\xi_{k,0}^{\text{MMSE}}$  and  $\xi_k^{\text{MMSE}}$  are obtained by substituting the optimum MMSE equalizers  $g_{k,0}^*$ ,  $g_k^*$  and the optimum MMSE weights  $w_{k,0}^*$ ,  $w_k^*$  back to the WMSEs. The optimum MMSE equalizers are  $g_{k,0}^* = g_{k,0}^{\text{MMSE}}$  and  $g_k^* = g_k^{\text{MMSE}}$  and the optimum MMSE weights are  $w_{k,0}^* = w_{k,0}^{\text{MMSE}} \triangleq (\varepsilon_{k,0}^{\text{MMSE}})^{-1}$  and  $w_k^* = w_k^{\text{MMSE}} \triangleq (\varepsilon_k^{\text{MMSE}})^{-1}$ . They are derived by checking the first order optimality conditions.

Based on the Rate-WMMSE relationships in (25), problem (20) is equivalently transformed into the WMMSE problem

$$\min_{\mathbf{P}, \mathbf{x}, \mathbf{w}, \mathbf{g}} \sum_{k \in \mathcal{K}} u_k \xi_{k,tot} \quad (26a)$$

$$\text{s.t. } X_{k,0} + \xi_{k,0} \leq 1 - R_k^{th}, \forall k \in \mathcal{K} \quad (26b)$$

$$X_0 + \sum_{k \in \mathcal{K}} X_{k,0} + 1 \geq \xi_{k,0}, \forall k \in \mathcal{K} \quad (26c)$$

$$X_0 \leq -R_0^{th} \quad (26d)$$

$$X_{k,0} \leq 0, \forall k \in \mathcal{K} \quad (26e)$$

$$\text{tr}(\mathbf{P}\mathbf{P}^H) \leq P_t \quad (26f)$$

where  $\mathbf{x} = [X_0, X_{1,0}, \dots, X_{K,0}]$  is the transformation of the common rate  $\mathbf{c}$ .  $\mathbf{w} = [w_{1,0}, \dots, w_{K,0}, w_1, \dots, w_K]$  and  $\mathbf{g} = [g_{1,0}, \dots, g_{K,0}, g_1, \dots, g_K]$  are the weights and equalizers, respectively.  $\xi_{k,tot} = X_{k,0} + \xi_k, \forall k \in \mathcal{K}$ .

Denote  $\mathbf{w}^{\text{MMSE}}$  and  $\mathbf{g}^{\text{MMSE}}$  as two vectors formed by the corresponding optimum MMSE equalizers and weights obtained by minimizing (26a) with respect to  $\mathbf{w}$  and  $\mathbf{g}$ , respectively.  $(\mathbf{w}^{\text{MMSE}}, \mathbf{g}^{\text{MMSE}})$  satisfies the Karush-Kuhn-Tucker (KKT) conditions of problem (26). Based on (25) and the common rate transformation  $\mathbf{c} = -\mathbf{x}$ , problem (26) can be transformed to problem (20). The solution given by  $(\mathbf{c}^* = -\mathbf{x}^*, \mathbf{P}^*)$  meets the KKT optimality conditions of (20) for any point  $(\mathbf{x}^*, \mathbf{P}^*, \mathbf{w}^*, \mathbf{g}^*)$  satisfying the KKT optimality conditions of (26). Hence, (20) and (26) are equivalent.

Though the joint optimization of  $(\mathbf{x}, \mathbf{P}, \mathbf{w}, \mathbf{g})$  in (26) is still non-convex, (26) is convex in each block of  $(\mathbf{x}, \mathbf{P})$ ,  $\mathbf{w}$ ,  $\mathbf{g}$  by fixing the other two blocks. The block-wise convexity of (26) motivates us to use the Alternating Optimization (AO) algorithm to solve the problem. Algorithm 1 specifies the detailed steps of AO.  $(\mathbf{w}, \mathbf{g})$  and  $(\mathbf{x}, \mathbf{P})$  are updated iteratively until the convergence of the WSR.  $\text{WSR}^{[n]}$  is the WSR calculated based on the updated  $(\mathbf{x}, \mathbf{P})$  at iteration  $[n]$ . The convergence of the AO algorithm is guaranteed since  $\text{WSR}^{[n]}$  is increasing with  $n$  and it is bounded above for a given power constraint. Note that the initialization of  $\mathbf{P}$  will influence the

---

**Algorithm 1: WMMSE-based AO algorithm**


---

```

1 Initialize:  $n \leftarrow 0$ ,  $\mathbf{P}^{[n]}$ ,  $\text{WSR}^{[n]}$ ;
2 repeat
3    $n \leftarrow n + 1$ ;
4    $\mathbf{P}^{[n-1]} \leftarrow \mathbf{P}$ ;
5    $\mathbf{w} \leftarrow \mathbf{w}^{\text{MMSE}}(\mathbf{P}^{[n-1]})$ ;  $\mathbf{g} \leftarrow \mathbf{g}^{\text{MMSE}}(\mathbf{P}^{[n-1]})$ ;
6   update  $(\mathbf{x}, \mathbf{P})$  by solving (26) using the updated  $\mathbf{w}, \mathbf{g}$ ;
7 until  $|\text{WSR}^{[n]} - \text{WSR}^{[n-1]}| \leq \epsilon$ ;

```

---

point of convergence due to the non-convexity of the problem. Global optimality of the solution cannot be guaranteed.

When CSIT is imperfect, the sampling-based method proposed in [23] is adopted to approximate the average rate over the CSIT error distribution for a given channel state estimate. The precoders are designed to maximize the average rate by using the optimization framework described above.

Similarly, problem (8), (13) and (16) are solved by respectively reformulating them into the equivalent WMMSE problem and using the corresponding AO algorithm to solve them.

### B. SCA-based algorithm for EE problems

The SCA-based algorithm to solve the two-user EE maximization problem of RS without individual QoS rate constraints in the unicast-only transmission is proposed in [20]. It is extended to solve the EE maximization problems in the non-orthogonal unicast and multicast transmission. We firstly explain the procedure to solve the RS problem (21) and then specify how (9), (14), (17) are solved correspondingly.

Comparing with the EE optimization problem (9) in [20], the main difference of the RS problem (21) in the non-orthogonal unicast and multicast transmission lies in the introduced QoS rate constraints (20b) and the multicast rate  $C_0$  in (20a), (20c), (20d). Similar as [20], we first use scalar variables  $\omega^2$ ,  $z$  and  $t$ , respectively to represent the WSR, total power consumption and EE metric, then problem (21) is equivalently transformed into

$$\max_{\mathbf{P}, \mathbf{w}, \omega, z, t} t \quad (27a)$$

$$\text{s.t. } \frac{\omega^2}{z} \geq t \quad (27b)$$

$$u_0 C_0 + \sum_{k \in \mathcal{K}} u_k (C_{k,0} + R_k) \geq \omega^2 \quad (27c)$$

$$z \geq \frac{1}{\eta} \text{tr}(\mathbf{P}\mathbf{P}^H) + P_{\text{cir}} \quad (27d)$$

$$(20b) - (20f) \quad (27e)$$

The equivalence between (27) and (21) is established based on the fact that (27b)–(27d) hold with equality at optimum.

By introducing variables  $\boldsymbol{\alpha} = [\alpha_1, \dots, \alpha_K]^T$ , constraints (20b) and (27c) become

$$C_{k,0} + \alpha_k \geq R_k^{th}, \forall k \in \mathcal{K} \quad (28a)$$

$$(20b), (27c) \Leftrightarrow u_0 C_0 + \sum_{k \in \mathcal{K}} u_k (C_{k,0} + \alpha_k) \geq \omega^2 \quad (28b)$$

$$R_k \geq \alpha_k, \forall k \in \mathcal{K} \quad (28c)$$

By adding variables  $\boldsymbol{\vartheta} = [\vartheta_1, \dots, \vartheta_K]^T$ , the rate constraint (28c) is transformed into

$$(28c) \Leftrightarrow \begin{cases} \vartheta_k \geq 2^{\alpha_k}, \forall k \in \mathcal{K} \\ 1 + \gamma_k \geq \vartheta_k, \forall k \in \mathcal{K} \end{cases} \quad (29a)$$

$$(29b)$$

By further introducing  $\beta = [\beta_1, \dots, \beta_K]^T$  to represent the interference plus noise at each user to decode its private stream, constraint (29b) is transformed into

$$(29b) \Leftrightarrow \begin{cases} \frac{|\mathbf{h}_k^H \mathbf{p}_k|^2}{\beta_k} \geq \vartheta_k - 1, \forall k \in \{1, 2\} \\ \beta_k \geq \sum_{j \neq k} |\mathbf{h}_k^H \mathbf{p}_j|^2 + 1, \forall k \in \{1, 2\} \end{cases} \quad (30a)$$

Therefore, constraints (20b) and (27c) are equivalent to

$$(20b), (27c) \Leftrightarrow (28a), (28b), (29a), (30)$$

The same method is used to transform constraint (20d). By introducing variable sets  $\alpha_0 = [\alpha_{1,0}, \dots, \alpha_{K,0}]^H$ ,  $\vartheta_0 = [\vartheta_{1,0}, \dots, \vartheta_{K,0}]^T$ ,  $\beta_0 = [\beta_{1,0}, \dots, \beta_{K,0}]^T$ , (20d) becomes

$$(20d) \Leftrightarrow \begin{cases} C_0 + \sum_{k \in \mathcal{K}} C_{k,0} \leq \alpha_{k,0}, \forall k \in \mathcal{K} \\ \vartheta_{k,0} \geq 2^{\alpha_{k,0}}, \forall k \in \mathcal{K} \\ \frac{|\mathbf{h}_k^H \mathbf{p}_0|^2}{\beta_{k,0}} \geq \vartheta_{k,0} - 1, \forall k \in \mathcal{K} \\ \beta_{k,0} \geq \sum_{j \in \mathcal{K}} |\mathbf{h}_k^H \mathbf{p}_j|^2 + 1 \end{cases} \quad (31a), (31b), (31c), (31d)$$

Therefore, problem (21) is equivalently transformed into

$$\begin{aligned} & \max_{\mathbf{c}, \mathbf{P}, \omega, z, t} && t \\ & \text{s.t.} && (20c), (20e), (20f), (27b), (27d) \\ & && (28a), (28b), (29a), (30), (31) \end{aligned}$$

However, constraints (27b), (30a) and (31c) are non-convex. Linear approximation methods adopted in [20] is used to approximate the non-convex part of the constraints in each iteration. Left side of (27b) is approximated at the point  $(\omega^{[n]}, z^{[n]})$  of the  $n$ th iteration by  $\frac{\omega^2}{z} \geq \frac{2\omega^{[n]}}{z^{[n]}}\omega - (\frac{\omega^{[n]}}{z^{[n]}})^2 z \triangleq \Omega^{[n]}(\omega, z)$ . The left side of (30a) is approximated at the point  $(\mathbf{p}_k^{[n]}, \beta_k^{[n]})$  as  $|\mathbf{h}_k^H \mathbf{p}_k|^2 / \beta_k \geq 2\text{Re}((\mathbf{p}_k^{[n]})^H \mathbf{h}_k \mathbf{h}_k^H \mathbf{p}_k) / \beta_k^{[n]} - (|\mathbf{h}_k^H \mathbf{p}_k^{[n]}| / \beta_k^{[n]})^2 \beta_k \triangleq \Psi_k^{[n]}(\mathbf{p}_k, \beta_k)$ . Similarly, the left side of (31c) is approximated at the point  $(\mathbf{p}_0^{[n]}, \beta_{k,0}^{[n]})$  by  $\Psi_{k,0}^{[n]}(\mathbf{p}_0, \beta_{k,0}) = 2\text{Re}((\mathbf{p}_0^{[n]})^H \mathbf{h}_k \mathbf{h}_k^H \mathbf{p}_0) / \beta_{k,0}^{[n]} - (|\mathbf{h}_k^H \mathbf{p}_0^{[n]}| / \beta_{k,0}^{[n]})^2 \beta_{k,0}$ .

Based on the above approximations, problem (21) is approximated at iteration  $n$  as

$$\begin{aligned} & \max_{\mathbf{c}, \mathbf{P}, \omega, z, t} && t \\ & \text{s.t.} && \Omega^{[n]}(\omega, z) \geq t \\ & && \Psi_k^{[n]}(\mathbf{p}_k, \beta_k) \geq \vartheta_k - 1, \forall k \in \mathcal{K} \\ & && \Psi_{k,0}^{[n]}(\mathbf{p}_0, \beta_{k,0}) \geq \vartheta_{k,0} - 1, \forall k \in \mathcal{K} \\ & && (20c), (20e), (20f), (28a), (28b), (29a), \\ & && (30b), (31a), (31b), (31d) \end{aligned} \quad (32)$$

Problem (32) is convex and can be solved using CVX in Matlab [27]. The details of the SCA-based algorithm is specified in Algorithm 2. In each iteration  $[n]$ , the approximate problem (32) defined around the solution of iteration  $[n-1]$  is solved.

*Initialization:* The precoder  $\mathbf{P}^{[0]}$  is initialized by solving

---

### Algorithm 2: SCA-based beamforming algorithm

---

- 1 **Initialize:**  $n \leftarrow 0$ ,  $t^{[n]}, \omega^{[n]}, z^{[n]}, \mathbf{P}^{[n]}, \beta_0^{[n]}, \beta^{[n]}$ ;
- 2 **repeat**
- 3      $n \leftarrow n + 1$ ;
- 4     Solve (32) using  $\omega^{[n-1]}, z^{[n-1]}, \mathbf{P}^{[n-1]}, \beta_0^{[n-1]}, \beta^{[n-1]}$  and denote the optimal values as  $\omega^*, z^*, \mathbf{P}^*, \beta_0^*, \beta^*$ ;
- 5     Update  $t^{[n]} \leftarrow t^*$ ,  $\omega^{[n]} \leftarrow \omega^*$ ,  $z^{[n]} \leftarrow z^*$ ,  $\mathbf{P}^{[n]} \leftarrow \mathbf{P}^*$ ,  $\beta_0^{[n]} \leftarrow \beta_0^*$ ,  $\beta^{[n]} \leftarrow \beta^*$ ;
- 6 **until**  $|t^{[n]} - t^{[n-1]}| < \epsilon$ ;

---

$$\text{find } \mathbf{P} \quad (33a)$$

$$\text{s.t. } R_k \geq R_k^{th}, \forall k \in \mathcal{K} \quad (33b)$$

$$R_{k,0} \geq R_{k,0}^{th}, \forall k \in \mathcal{K} \quad (33c)$$

$$\text{tr}(\mathbf{P} \mathbf{P}^H) \leq P_t \quad (33d)$$

where we assume the supper-common stream only includes the multicast stream while the unicast streams are transmitted using the private streams.  $C_0 = R_0$ ,  $C_{k,0} = 0, \forall k$ . According to the SINR constraint transformation in [28], constraints (33b) and (33c) can be transformed into

$$(33b), (33c) \Leftrightarrow \begin{cases} \frac{1}{\sqrt{2R_k^{th}}} \mathbf{h}_k^H \mathbf{p}_k \geq \sqrt{\sum_{j \neq k} |\mathbf{h}_k^H \mathbf{p}_j|^2 + 1}, \forall k \in \mathcal{K} \\ \frac{1}{\sqrt{2R_{k,0}^{th}}} \mathbf{h}_k^H \mathbf{p}_0 \geq \sqrt{\sum_{j \in \mathcal{K}} |\mathbf{h}_k^H \mathbf{p}_j|^2 + 1}, \forall k \in \mathcal{K} \end{cases} \quad (34)$$

Based on (34), problem (33) becomes a Second Order Cone Problem (SOCP) feasibility problem and can be solved by the standard solvers in MatLab.  $\omega^{[0]}, z^{[0]}, \beta_k^{[0]}$  and  $\beta_{k,0}^{[0]}$  are initialized by respectively replacing the inequalities of (27c), (27d), (30b) and (31d) with equalities.

*Convergence Analysis:* The solution of problem (32) in iteration  $[n]$  is also a feasible solution of the problem in iteration  $[n+1]$  since the approximated problem (32) in iteration  $[n+1]$  is defined around the solution of iteration  $[n]$ . Hence, the EE objective  $t^{[n+1]}$  is larger than or equal to  $t^{[n]}$ . In other words, Algorithm 2 generates a nondecreasing sequence of objective values. Moreover, the EE objective  $t$  is bounded above by the transmit power constraint. We conclude that Algorithm 2 is guaranteed to converge while the global optimality of the achieved solution can not be guaranteed.

Problems (9), (14), (17) are solved by respectively approximating them using the above transformation and approximation, which are then solved iteratively by the corresponding SCA-based beamforming algorithm as well.

## VII. NUMERICAL RESULTS OF WSR PROBLEM

In this section, we evaluate the WSR of all the transmission strategies in various user deployments and network loads.

### A. Two-user deployments

In the two-user deployments, the influence of different channel strength disparities, channel angles between the users, CSIT inaccuracy and the multicast rate constraints on the performance are investigated. We compare MU-LP, SC-SIC and RS-based transmission strategies. Note that SC-SIC per group is not investigated in the two-user deployments since

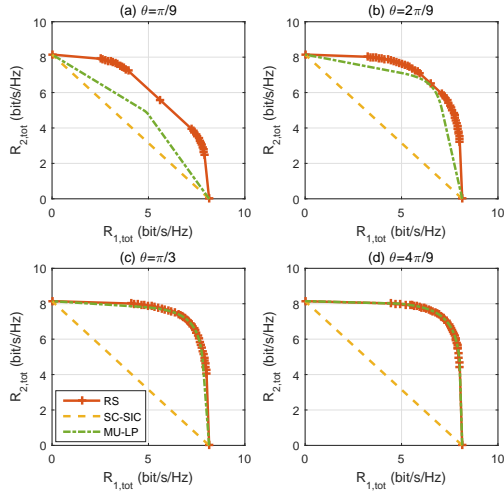


Fig. 2: Achievable rate region comparison of different strategies in perfect CSIT,  $\gamma = 1$ ,  $R_0^{th} = 0.5$  bit/s/Hz,  $R_k^{th} = 0$ ,  $\forall k$ .

two layers of SIC are required at each user in the two-user SC-SIC per group. There is no need to use one additional layer of SIC at each user to separate the multicast stream and the unicast stream to be decoded by both users before decoding the unicast streams. In contrast to SC-SIC per group, the receiver complexities of MU-LP, SC-SIC and RS-assisted strategies are the same when  $K = 2$ . One layer of SIC is required.

1) *Perfect CSIT*: We assume the BS has four antennas ( $N_t = 4$ ) and serves two single-antenna users. Following the two-user deployment in [13], the channels of the users are realized as  $\mathbf{h}_1 = [1, 1, 1, 1]^H$ ,  $\mathbf{h}_2 = \gamma \times [1, e^{j\theta}, e^{j2\theta}, e^{j3\theta}]^H$ .  $\gamma$  controls the channel gain difference between user-1 and user-2.  $\gamma = 1$  and  $\gamma = 0.3$  represent equal channel strength and 10 dB channel strength difference, respectively. For each  $\gamma$ , we consider  $\theta \in [\frac{\pi}{9}, \frac{2\pi}{9}, \frac{\pi}{3}, \frac{4\pi}{9}]$ . The user channels are sufficiently aligned when  $0 < \theta < \frac{\pi}{9}$  while the channels are sufficiently orthogonal when  $\frac{4\pi}{9} < \theta < \frac{\pi}{2}$ . The boundary of the rate region is the set of achievable points calculated by solving the WSR maximization problem with various weights assigned to users. The weight of user-1 is fixed to  $u_1 = 1$  for each weight of user-2 in  $u_2 \in 10^{[-3, -1, -0.95, \dots, 0.95, 1, 3]}$  as used in [13]. The initialization of precoders follows the methods used in [13], [23]. SNR is fixed to 20 dB. To investigate the largest achievable rate region of the unicast streams, the unicast rate constraints are set to 0 in all strategies  $R_k^{th} = 0$ ,  $\forall k \in \{1, 2\}$ .

Fig. 2–4 show the achievable rate region comparison of different strategies in perfect CSIT. In all figures, the rate region of RS is confirmed to be equal to or larger than that of SC-SIC and MU-LP. RS performs well for any channel strength disparity as well as any angle between the user channels. In contrast, SC-SIC and MU-LP are sensitive to the channel strength disparities and channel angles. In each figure, RS exhibits a clear rate region improvement over MU-LP when the user channels are closely aligned. As  $\theta$  increases, the rate region gap between RS and MU-LP decreases and RS reduces to MU-LP when  $\theta = \frac{4\pi}{9}$ . This is due to the fact that the precoder of MU-LP mitigates co-channel interference by utilizing the spatial separation among users. When the user channels are aligned, the interference-nulling will lose efficacy.

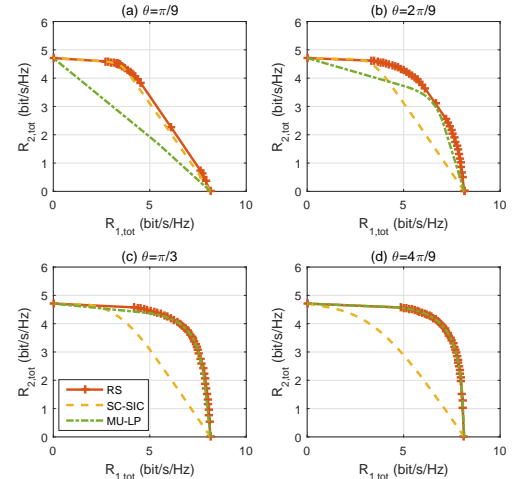


Fig. 3: Achievable rate region comparison of different strategies in perfect CSIT,  $\gamma = 0.3$ ,  $R_0^{th} = 0.5$  bit/s/Hz,  $R_k^{th} = 0$ ,  $\forall k$ .

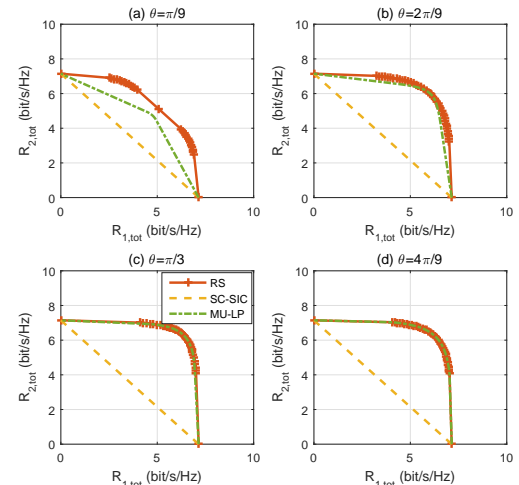


Fig. 4: Achievable rate region comparison of different strategies in perfect CSIT,  $\gamma = 1$ ,  $R_0^{th} = 1.5$  bit/s/Hz,  $R_k^{th} = 0$ ,  $\forall k$ .

Comparing the corresponding subfigures of Fig. 2 and Fig. 3, the rate region of SC-SIC is closer to that of RS only when there is a 10 dB channel strength disparity and the user channels are aligned. Since SC-SIC is motivated by leveraging the users' channel strength disparity in SISO BC, it is sensitive to the channel strength disparity as well as channel angles. When the users have similar channel strengths or (semi-)orthogonal channel angles, the performance of SC-SIC is much worse than RS. Comparing with MU-LP and SC-SIC, RS is more robust to a wide range of channel gain difference and channel angles among users. This performance gain comes at no additional cost for the receivers since one layer of SIC is also required for MU-LP and SC-SIC in the two-user deployments.

As the multicast rate constraint  $R_0^{th}$  increases, the rate region of each strategy decreases. This can be observed by comparing the corresponding subfigures of Fig. 2 and Fig. 4. However, the rate region gaps among the three strategies decrease when  $R_0^{th}$  increases since a larger portion of the power is used for transmitting the multicast stream via the super-common stream. RS achieves a better unicast rate region than MU-LP and SC-SIC when a larger portion of the transmit power is

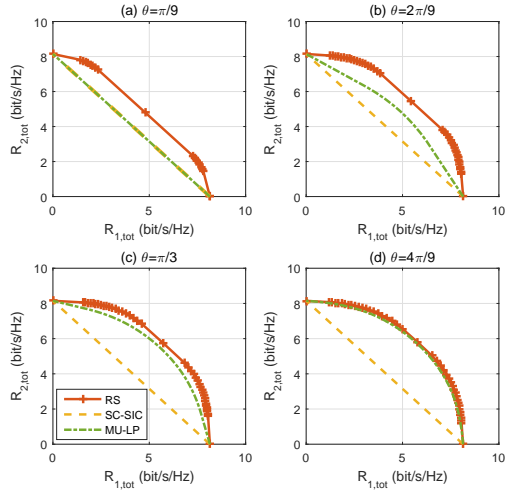


Fig. 5: Average rate region comparison of different strategies in imperfect CSIT,  $\gamma = 1$ ,  $R_0^{th} = 0.5$  bit/s/Hz,  $R_k^{th} = 0, \forall k$ .

allocated to the unicast streams. Adequate power allocation for the unicast streams allows RS to better determine the level of the interference to decode and treat as noise.

2) *Imperfect CSIT*: When CSIT is imperfect, the estimated channels of user-1 and user-2 are realized as  $\hat{\mathbf{h}}_1 = [1, 1, 1, 1]^H$  and  $\hat{\mathbf{h}}_2 = \gamma \times [1, e^{j\theta}, e^{j2\theta}, e^{j3\theta}]^H$ , respectively. The precoders are initialized and designed using the estimated channels  $\hat{\mathbf{h}}_1, \hat{\mathbf{h}}_2$  and the same methods as stated in [13], [23]. The real channel realization is obtained as  $\mathbf{h}_k = \hat{\mathbf{h}}_k + \tilde{\mathbf{h}}_k, \forall k \in \{1, 2\}$ , where  $\tilde{\mathbf{h}}_k$  is the estimation error of user- $k$  with independent and identically distributed (i.i.d.) complex Gaussian entries drawn from  $\mathcal{CN}(0, \sigma_{e,k}^2)$ . The error covariances of user-1 and user-2 are  $\sigma_{e,1}^2 = P_t^{-0.6}$  and  $\sigma_{e,2}^2 = \gamma P_t^{-0.6}$ , respectively. The unicast rate constraints are set to 0 in all strategies  $R_k^{th} = 0, \forall k \in \{1, 2\}$ . Other unspecified parameters remain consistent with perfect CSIT results. After generating 1000 different channel error samples for each user, each point in the rate region is the average rate over the resulting 1000 channels. Note that the average rate is a short-term (instantaneous) measure that captures the expected performance over the CSIT error distribution for a given channel state estimate [23].

Fig. 5–6 show the results when  $R_0^{th} = 0.5$  bit/s/Hz in imperfect CSIT,  $\gamma = 1$  and  $\gamma = 0.3$ , respectively. Comparing the corresponding figures of perfect and imperfect CSIT (Fig. 2 and Fig. 5, Fig. 3 and Fig. 6), we conclude that the rate region gap between RS and MU-LP increases in imperfect CSIT. This is due to the fact that the interference nulling in MU-LP is distorted and the residual interference at the receiver deteriorates the achievable rate. When  $\gamma = 0.3$ , the rate region gap between RS and SC-SIC is reduced in imperfect CSIT, though it is still obvious especially when the channels are (semi-)orthogonal. Comparing with MU-LP and SC-SIC, RS is more robust to a wide range of CSIT inaccuracy, channel gain difference and channel angles among users. The transmit scheduler of RS is simpler as it copes with any user deployment scenarios. RS always outperforms MU-LP and SC-SIC.

### B. Three-user deployments

To exploit the benefits of the linearly precoded RS, we also apply the generalized RS model proposed in [13] to the non-

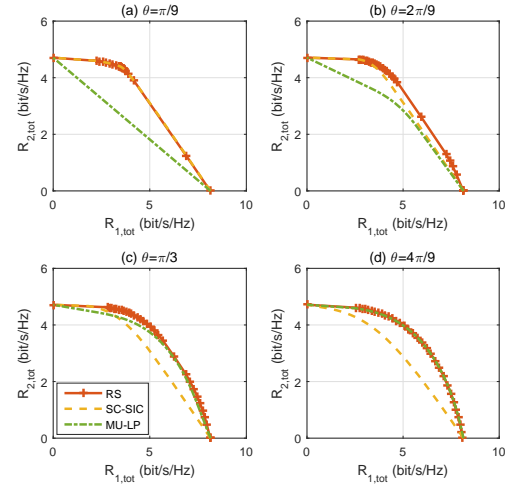


Fig. 6: Average rate region comparison of different strategies in imperfect CSIT,  $\gamma = 0.3$ ,  $R_0^{th} = 0.5$  bit/s/Hz,  $R_k^{th} = 0, \forall k$ .

orthogonal unicast and multicast transmission. When  $K = 3$ , there will be two layers of common streams in the generalized RS model. Each user requires three layers of SIC to decode all the intended streams. In the following results of WSR performance, the term 'RS' is used to represent the generalized RS model in [13] while '1-layer RS' refers to the RS model in Section V. Comparing the receiver complexities, RS requires three layers of SIC at each user. Both SC-SIC and SC-SIC per group require two layers of SIC at each user while MU-LP and 1-layer RS only need one layer of SIC. The receiver complexities of MU-LP and 1-layer RS are the lowest.

In the three-user deployments, we further investigate the influence of different network loads and SNR values on the WSR performance. We compare MU-LP, SC-SIC, SC-SIC per group, 1-layer RS and the generalized RS transmission strategies. In SC-SIC per group, the grouping method and decoding order are required to be jointly optimized with the precoder in order to maximize the WSR, which results in very high computational burden at the BS as the number of user increases. To reduce the complexity of SC-SIC per group, we consider a fixed grouping method. We assume user-1 is in group-1 while user-2 and user-3 are in group-2. The decoding order will be optimized together with the precoder.

1) *Perfect CSIT*: Following the precoder initialization and channel realizations for three-user deployments in [13], we consider specific channel realizations given by  $\mathbf{h}_1 = [1, 1, 1, 1]^H$ ,  $\mathbf{h}_2 = \gamma_1 \times [1, e^{j\theta_1}, e^{j2\theta_1}, e^{j3\theta_1}]^H$ ,  $\mathbf{h}_3 = \gamma_2 \times [1, e^{j\theta_2}, e^{j2\theta_2}, e^{j3\theta_2}]^H$  for the underloaded three-user deployments ( $N_t = 4$ ). For the overloaded three-user deployments ( $N_t = 2$ ), the channels are realized as  $\mathbf{h}_1 = [1, 1]^H$ ,  $\mathbf{h}_2 = \gamma_1 \times [1, e^{j\theta_1}]^H$ ,  $\mathbf{h}_3 = \gamma_2 \times [1, e^{j\theta_2}]^H$ .  $\gamma_1, \gamma_2$  and  $\theta_1, \theta_2$  are control variables. We assume user-1 and user-2 have equal channel strength ( $\gamma_1 = 1$ ) and there is a 10 dB channel gain difference between user-1/user-2 and user-3 ( $\gamma_2 = 0.3$ ). For the given set of  $\gamma_1, \gamma_2$ ,  $\theta_1$  adopts value from  $\theta_1 = [\frac{\pi}{9}, \frac{2\pi}{9}, \frac{\pi}{3}, \frac{4\pi}{9}]$  and  $\theta_2 = 2\theta_1$ . In all the three-user results, the weights of the users are assumed to be equal to  $u_1 = u_2 = u_3 = 1$ . The QoS rate requirements of the multicast and unicast streams are assumed to be equal and the rate threshold is increas-

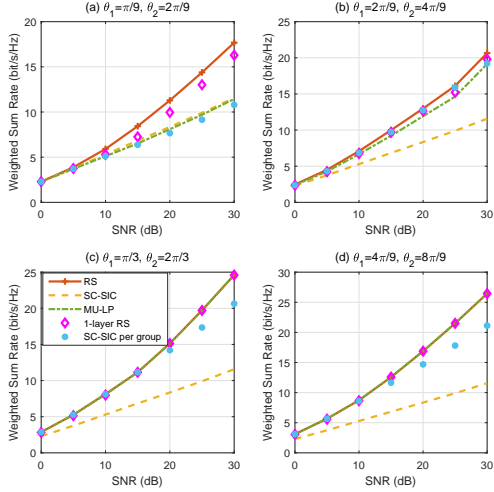


Fig. 7: WSR versus SNR comparison of different strategies for underloaded three-user deployment in perfect CSIT,  $\gamma_1 = 1, \gamma_2 = 0.3, N_t = 4$ .

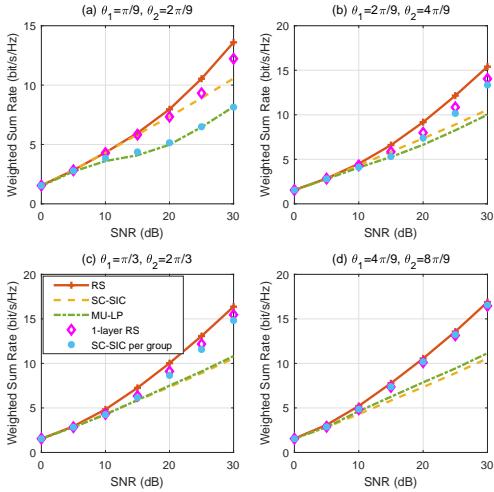


Fig. 8: WSR versus SNR comparison of different strategies for overloaded three-user deployment in perfect CSIT,  $\gamma_1 = 1, \gamma_2 = 0.3, N_t = 2$ .

ing with SNR. For  $\text{SNR} = [0, 5, 10, 15, 20, 25, 30]$  dBs, the corresponding rate constraint vector of stream- $j$  is  $\mathbf{r}_j^{th} = [0.005, 0.01, 0.05, 0.15, 0.3, 0.4, 0.4] \text{ bit/s/Hz}, \forall j \in \{0, 1, 2, 3\}$ .

Fig. 7 and Fig. 8 show the results of WSR versus SNR comparison of different strategies in perfect CSIT for the underloaded and overloaded three-user deployments, respectively. RS exhibits a clear WSR gain over 1-layer RS, MU-LP, SC-SIC, SC-SIC per group in both figures. 1-layer RS achieves a more stable performance than MU-LP, SC-SIC, SC-SIC per group as the channel strength disparity and channel angles among users changes. The WSR performance of MU-LP deteriorates as the channel angles among users become smaller (aligned) or the network loads become overloaded. In contrast, the WSR performance of SC-SIC deteriorates as the channel angles among users becomes larger or the network load becomes underloaded. SC-SIC per group compensates the shortcomings of SC-SIC. It achieves a better performance than SC-SIC for orthogonal channels or underloaded network loads

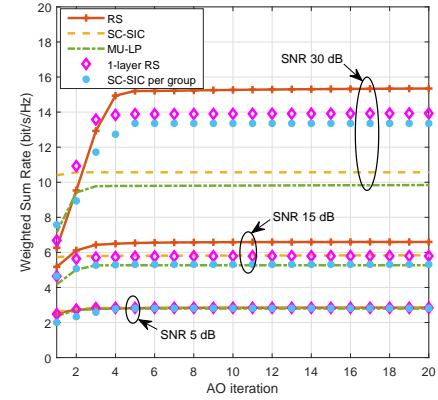


Fig. 9: WSR convergence of Algorithm 1 with different transmission strategies,  $\theta_1 = \frac{2\pi}{9}, \theta_2 = \frac{4\pi}{9}, N_t = 2$ .

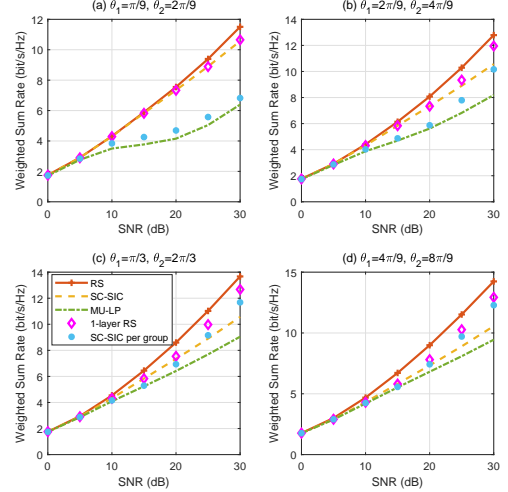


Fig. 10: WSR versus SNR comparison of different strategies for overloaded three-user deployment in imperfect CSIT,  $\gamma_1 = 1, \gamma_2 = 0.3, N_t = 2$ .

as it allows the inter-group interference to be treated as noise. Thanks to the ability of partially decoding the interference and partially treating the interference as noise, RS and 1-layer RS are less sensitive to the user channel orthogonality as well as the network loads. Considering the trade-off between performance and complexity, 1-layer RS is the best choice since it has the lowest receiver complexity and a more robust performance over various user deployments and network loads.

The convergence rates of all considered transmission strategies for a specific channel realization are analyzed in Fig. 9. The rate constraints of all the streams are equal to the corresponding value in  $\mathbf{r}_j^{th}$  for a given SNR (i.e. when  $\text{SNR} = 5 \text{ dB}, R_j^{th} = 0.01 \text{ bit/s/Hz}, \forall j \in \{0, 1, 2, 3\}$ ). As the decoding orders in RS, SC-SIC and SC-SIC per group are required to be optimized with the precoders, the convergence rate of the optimal decoding order that achieves the highest WSR for the corresponding transmission strategy is illustrated in Fig. 9. For various SNR values, a few iterations are required for each strategy to converge. The convergence rate slightly increases with SNR since the overall optimization space is enlarged.

2) *Imperfect CSIT*: In the imperfect CSIT scenario, the precoder initialization and channel realizations follow the meth-

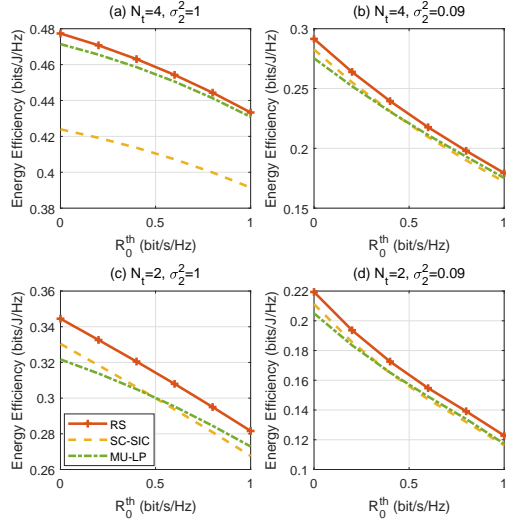


Fig. 11: Energy Efficiency versus  $R_0^{th}$  comparison of different strategies for two-user deployment in perfect CSIT, averaged over 100 random channels.  $R_1^{th} = R_2^{th} = 0.5$  bit/s/Hz, SNR=10 dB,  $u_0 = u_1 = u_2 = 1$ .

ods discussed in the two-user deployment of Section VII-A2. Readers are also referred to Appendix E in [13] for more details. Other unspecified parameters remain consistent with the perfect CSIT scenarios of Section VII-B1.

Fig. 10 shows the results of WSR versus SNR comparison in the overloaded three-user deployment with imperfect CSIT. Comparing Fig. 8 and Fig. 10, the WSR gap between RS and SC-SIC per group/MU-LP is enlarged when the CSIT becomes imperfect. SC-SIC per group and MU-LP are sensitive to the CSIT inaccuracy. Though 1-layer RS has the lowest receiver complexity, it achieves a better WSR than SC-SIC, SC-SIC per group and MU-LP in all the subfigures.

## VIII. NUMERICAL RESULTS OF EE PROBLEM

In this section, we evaluate the EE of all the transmission strategies in various user deployments and network loads.

### A. Two-user deployments

In the two-user deployment, we investigate the influence of different multicast rate constraints, channel strength disparities, channel angles between the users and the network loads on the EE performance. We compare the RS model in Section V, MU-LP, SC-SIC-assisted transmission strategies.

1) *Random channel realizations*: We firstly consider the scenarios when the channel of each user  $\mathbf{h}_k$  has i.i.d complex Gaussian entries with a certain variance, i.e.,  $\mathcal{CN}(0, \sigma_k^2)$ . The variance of entries of  $\mathbf{h}_1$  is fixed to 1 ( $\sigma_1^2 = 1$ ) while the variance of entries of  $\mathbf{h}_2$  is varied ( $\sigma_2^2 = 1, 0.09$ ). The BS is equipped with two or four antennas ( $N_t = 2, 4$ ) and serves two single-antenna users. Following the simulation parameters used in [20], the static power consumption is  $P_{sta} = 30$  dBm and the dynamic power consumption is  $P_{dyn} = 27$  dBm. The power amplifier efficiency is  $\eta = 0.35$ .

Fig. 11 shows the results of EE versus the multicast rate requirement  $R_0^{th}$  comparison of three transmission strategies for the two-user deployment with perfect CSIT. In all subfigures, the EEs of all the strategies decrease as  $R_0^{th}$  increases.

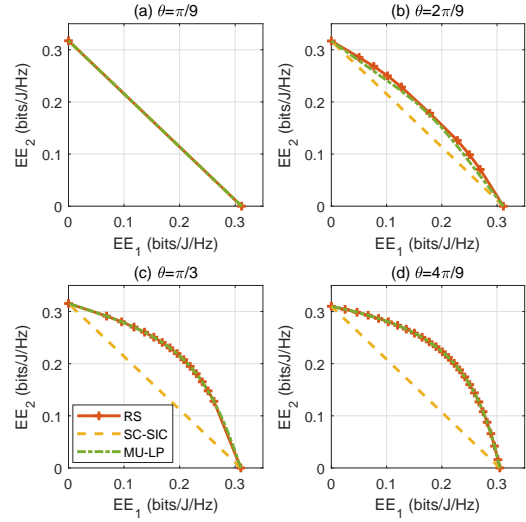


Fig. 12: Energy Efficiency region comparison of different strategies for two-user deployment in perfect CSIT,  $\gamma = 1$ .

When  $R_0^{th}$  is large, more power is allocated to satisfy the multicast rate requirement. The overall EE optimization space is shrunk. The proposed RS-assisted non-orthogonal unicast and multicast transmission outperforms SC-SIC and MU-LP in all the considered user deployments. Comparing subfigure (a) and (c), we observe that the EE gap between RS and MU-LP increases as the number of transmit antennas decreases. MU-LP achieves a better EE performance when the total number of transmit antennas is larger than the total number of receive antennas (underloaded regime). In contrast, SC-SIC performs better when the total number of transmit antennas is much less (overloaded regime). Such observation of the EE performance is consistent with that of the WSR performance.

2) *Specific channel realizations*: We further consider specific channel realizations based on the channel realizations and relevant simulation parameters specified in Section VII-A1. Different from the WSR problem where the objective is to maximize the WSR of the unicast streams, the considered EE problem maximizes the WSR of the multicast streams and the unicast streams. In order to investigate the EE region achieved by the unicast streams, the rate allocated to the multicast stream is fixed at  $R_0^{th}$ , i.e.,  $C_0 = R_0^{th}$ . In the following results, we assume  $R_0^{th} = 0.5$  bit/s/Hz and  $u_0 = 1$ . SNR is fixed at 10 dB and the transmitter is equipped with four tansmit antennas ( $N_t = 4$ ). The unspecified parameters remain the same as in the random channel realization section. The EE metric of each unicast stream is defined as the achievable unicast rate divided by the sum power. The individual EE of user- $k$  is  $EE_k = R_{k,tot}/(\frac{1}{\eta}\text{tr}(\mathbf{P}\mathbf{P}^H) + P_{cir}), \forall k \in \{1, 2\}$ .

Fig. 12 and Fig. 13 illustrate the EE region of different strategies for two-user deployment in perfect CSIT,  $\gamma = 1$  and  $\gamma = 0.3$ , respectively. The EE region of RS is always larger than or equal to the EE region of MU-LP or SC-SIC in both figures. The EE performance of MU-LP is superior when the user channels are sufficiently aligned. In contrast, the EE performance of SC-SIC is superior when there is a 10 dB channel gain difference or the user channels are aligned. Comparing with the EE regions of the unicast-only

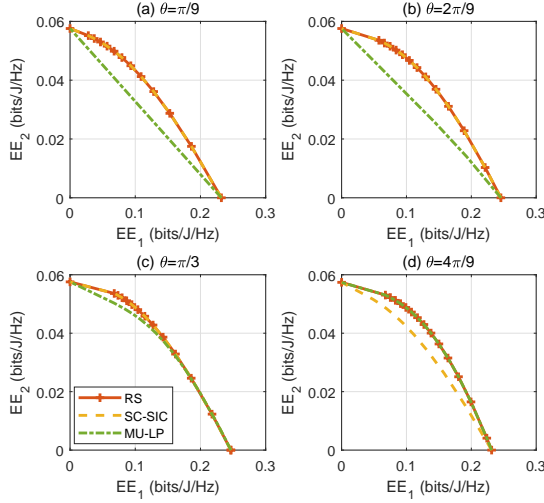


Fig. 13: Energy Efficiency region comparison of different strategies for two-user deployment in perfect CSIT,  $\gamma = 0.3$ .

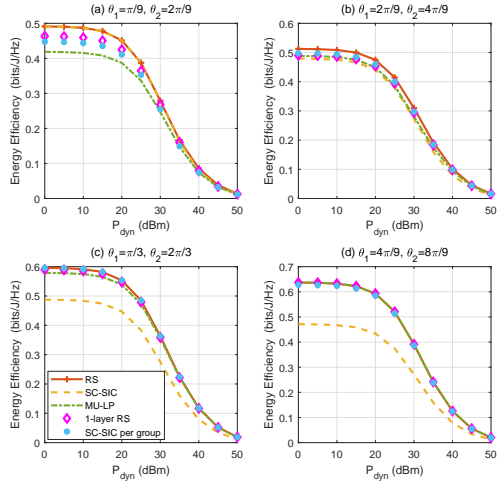


Fig. 14: Energy Efficiency versus  $P_{\text{dyn}}$  comparison of different strategies for underloaded three-user deployment in perfect CSIT,  $N_t = 4$ .

transmission illustrated in [20], the EE region improvement of RS in Fig. 12 and Fig. 13 is not obvious due to the introduced multicast stream. As discussed in Section VIII-A1, the overall optimization space is reduced since part of the power is allocated to the multicast stream so as to meet the multicast rate requirement.

### B. Three-user deployments

In the three-user deployment, we focus on the specific channel realizations and the influence of different  $P_{\text{dyn}}$  values on the EE performance is further investigated. Following the three-user WSR analysis, we compare the generalized RS transmission strategy proposed in [13] (denoted as 'RS' in the sequel), MU-LP, SC-SIC, SC-SIC per group and the proposed low-complexity RS (denoted as '1-layer RS' in the sequel) described in previous sections. The specific channel model specified in Section VII-B1 is used in this section. In the following results, the QoS rate constraints of the multicast and unicast streams are assumed to be equal to 0.1 bit/s/Hz, i.e.,  $R_0^{th} = R_1^{th} = R_2^{th} = R_3^{th} = 0.1$  bit/s/Hz. The weights

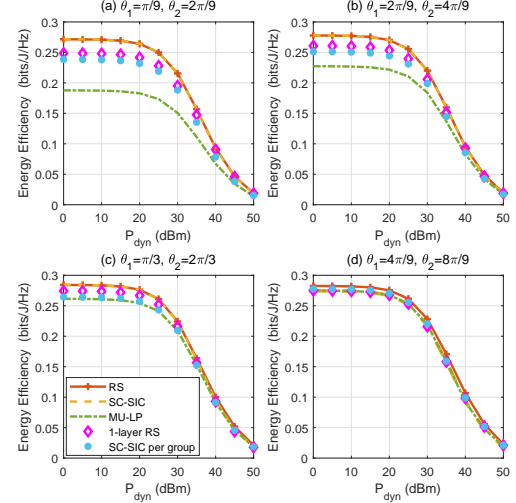


Fig. 15: Energy Efficiency versus  $P_{\text{dyn}}$  comparison of different strategies for overloaded three-user deployment in perfect CSIT,  $N_t = 2$ .

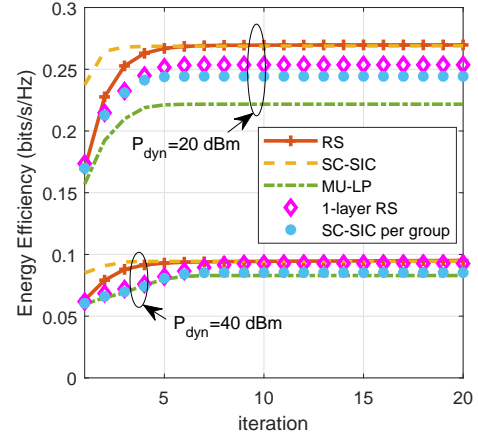


Fig. 16: EE convergence of Algorithm 2 with different transmission strategies,  $\theta_1 = \frac{2\pi}{9}$ ,  $\theta_2 = \frac{4\pi}{9}$ ,  $N_t = 2$ .

allocated to the streams are equal to one, i.e.,  $u_0 = u_1 = u_2 = u_3 = 1$ . SNR is fixed to 10 dB. The channel strength disparities are fixed to  $\gamma_1 = 1$ ,  $\gamma_2 = 0.3$ .

Fig. 14 and Fig. 15 illustrate the EE versus  $P_{\text{dyn}}$  comparison of different strategies for underloaded and overloaded three-user deployments with perfect CSIT, respectively. In both figures, the generalized RS always outperforms all other strategies. Though MU-LP and the proposed 1-layer RS have the lowest receiver complexity, the EE performance of 1-layer RS outperforms MU-LP in all figures. It achieves a better EE performance than SC-SIC per group in most simulated user deployments and network loads. 1-layer RS also outperforms SC-SIC when the user channels are sufficiently orthogonal. We conclude that 1-layer RS provides more robust EE performance than MU-LP, SC-SIC and SC-SIC per group towards different user deployments and network loads.

The EE convergence of all considered transmission strategies for a specific channel realization is analyzed in Fig. 16. For various dynamic power values  $P_{\text{dyn}}$ , a few iterations are required for each strategy to converge. Both MU-LP and 1-layer RS-assisted transmission strategies use Algorithm 2

just once to complete the optimization procedure. In contrast, Algorithm 2 is required to be repeated for each decoding order of RS/SC–SIC/SC–SIC per group-assisted strategies, which results in much higher computational burden at the transmitter especially when the number of served users is large. The proposed (1-layer) RS-assisted non-orthogonal unicast and multicast transmission achieves an excellent tradeoff between EE performance and complexity.

## IX. CONCLUSIONS

To conclude, we propose a linearly precoded RS-assisted non-orthogonal unicast and multicast transmission strategy and two NOMA-assisted transmission strategies, namely 'SC–SIC' and 'SC–SIC per group'. The precoders of all the strategies are designed by maximizing the WSR/EE subject to the sum power constraint and the QoS rate requirements of all the messages. Two low-complexity WMMSE-based and SCA-based optimization frameworks are proposed to solve the WSR and EE maximization problems, respectively. Numerical results show that the proposed RS-assisted strategy is more spectrally efficient and energy efficient than the existing MU–LP-assisted strategy in a wide range of user deployments (with a diversity of channel directions, channel strengths and qualities of channel state information at the transmitter) and network loads (underloaded and overloaded regimes). It also achieves a more robust WSR and EE performance than the proposed NOMA-assisted strategies. Most importantly, the high-quality performance of RS comes without any increase in the receiver complexity compared with MU–LP and the receiver complexity of RS is much lower than the proposed NOMA-based strategies. The one-layer SIC in RS is used for the dual purpose of separating the unicast and multicast streams as well as better managing the multi-user unicast interference. Hence, the benefits of SIC is further explored in the proposed RS-based strategy.

## REFERENCES

- [1] Y. Mao, B. Clerckx, and V. O. K. Li, "Rate-splitting for multi-antenna non-orthogonal unicast and multicast transmission," *arXiv preprint arXiv:1802.05567*, 2018.
- [2] D. Kim, F. Khan, C. V. Rensburg, Z. Pi, and S. Yoon, "Superposition of broadcast and unicast in wireless cellular systems," *IEEE Communications Magazine*, vol. 46, no. 7, pp. 110–117, July 2008.
- [3] U. Sethakaset and S. Sun, "Sum-rate maximization in the simultaneous unicast and multicast services with two users," in *21st Annual IEEE International Symposium on Personal, Indoor and Mobile Radio Communications*, Sept 2010, pp. 672–677.
- [4] Y. Jia, Z. Chen, and P. Ren, "User selection algorithms for simultaneous unicast and multicast services," in *2012 8th International Conference on Wireless Communications, Networking and Mobile Computing*, Sept 2012, pp. 1–4.
- [5] J. Zhao, O. Simeone, D. Gunduz, and D. Gomez-Barquero, "Non-orthogonal unicast and broadcast transmission via joint beamforming and LDM in cellular networks," in *2016 IEEE Global Communications Conference (GLOBECOM)*, Dec 2016, pp. 1–6.
- [6] Y. F. Liu, C. Lu, M. Tao, and J. Wu, "Joint multicast and unicast beamforming for the MISO downlink interference channel," in *2017 IEEE 18th International Workshop on Signal Processing Advances in Wireless Communications (SPAWC)*, July 2017, pp. 1–5.
- [7] E. Chen, M. Tao, and Y.-F. Liu, "Joint base station clustering and beamforming for non-orthogonal multicast and unicast transmission with backhaul constraints," *arXiv preprint arXiv:1712.01508*, 2017.
- [8] O. Tervo, L.-N. Tran, S. Chatzinotas, M. Junutti, and B. Ottersten, "Energy-efficient joint unicast and multicast beamforming with multi-antenna user terminals," *arXiv preprint arXiv:1705.03723*, 2017.
- [9] L. Zhang, W. Li, Y. Wu, X. Wang, S. I. Park, H. M. Kim, J. Y. Lee, P. Angueira, and J. Montalban, "Layered-division-multiplexing: Theory and practice," *IEEE Transactions on Broadcasting*, vol. 62, no. 1, pp. 216–232, March 2016.
- [10] D. Gmez-Barquero and O. Simeone, "LDM versus FDM/TDM for unequal error protection in terrestrial broadcasting systems: An information-theoretic view," *IEEE Transactions on Broadcasting*, vol. 61, no. 4, pp. 571–579, Dec 2015.
- [11] H. Weingarten, Y. Steinberg, and S. Shamai, "On the capacity region of the multi-antenna broadcast channel with common messages," in *2006 IEEE International Symposium on Information Theory*, July 2006, pp. 2195–2199.
- [12] Y. Geng and C. Nair, "The capacity region of the two-receiver gaussian vector broadcast channel with private and common messages," *IEEE Transactions on Information Theory*, vol. 60, no. 4, pp. 2087–2104, April 2014.
- [13] Y. Mao, B. Clerckx, and V. O. Li, "Rate-splitting multiple access for downlink communication systems: bridging, generalizing, and outperforming SDMA and NOMA," *EURASIP Journal on Wireless Communications and Networking*, vol. 2018, no. 1, p. 133, May 2018.
- [14] Y. Saito, Y. Kishiyama, A. Benjebbour, T. Nakamura, A. Li, and K. Higuchi, "Non-orthogonal multiple access (NOMA) for cellular future radio access," in *2013 IEEE 77th Vehicular Technology Conference (VTC Spring)*, June 2013, pp. 1–5.
- [15] Z. Ding, Z. Zhao, M. Peng, and H. V. Poor, "On the spectral efficiency and security enhancements of noma assisted multicast-unicast streaming," *IEEE Transactions on Communications*, vol. 65, no. 7, pp. 3151–3163, July 2017.
- [16] L. Yang, J. Chen, Q. Ni, J. Shi, and X. Xue, "NOMA-enabled cooperative unicast–multicast: Design and outage analysis," *IEEE Transactions on Wireless Communications*, vol. 16, no. 12, pp. 7870–7889, Dec 2017.
- [17] Z. Yang, J. A. Hussein, P. Xu, Z. Ding, and Y. Wu, "Power allocation study for non-orthogonal multiple access networks with multicast-unicast transmission," *IEEE Transactions on Wireless Communications*, Mar 2018.
- [18] B. Clerckx, H. Joudeh, C. Hao, M. Dai, and B. Rassouli, "Rate splitting for MIMO wireless networks: A promising PHY-layer strategy for LTE evolution," *IEEE Communications Magazine*, vol. 54, no. 5, pp. 98–105, May 2016.
- [19] H. Joudeh and B. Clerckx, "Rate-splitting for max-min fair multigroup multicast beamforming in overloaded systems," *IEEE Transactions on Wireless Communications*, vol. 16, no. 11, pp. 7276–7289, Nov 2017.
- [20] Y. Mao, B. Clerckx, and V. O. K. Li, "Energy efficiency of rate-splitting multiple access, and performance benefits over SDMA and NOMA," *arXiv preprint arXiv:arXiv:1804.08330*, 2018.
- [21] Y. Mao, B. Clerckx, and V. O. Li, "Rate-splitting multiple access for cooperative multi-cell networks," *arXiv preprint arXiv:1804.10516*, 2018.
- [22] C. Hao, Y. Wu, and B. Clerckx, "Rate analysis of two-receiver MISO broadcast channel with finite rate feedback: A rate-splitting approach," *IEEE Transactions on Communications*, vol. 63, no. 9, pp. 3232–3246, Sept 2015.
- [23] H. Joudeh and B. Clerckx, "Sum-rate maximization for linearly precoded downlink multiuser MISO systems with partial CSIT: A rate-splitting approach," *IEEE Transactions on Communications*, vol. 64, no. 11, pp. 4847–4861, Nov 2016.
- [24] M. Dai and B. Clerckx, "Multiuser millimeter wave beamforming strategies with quantized and statistical CSIT," *IEEE Transactions on Wireless Communications*, vol. 16, no. 11, pp. 7025–7038, Nov 2017.
- [25] H. Joudeh and B. Clerckx, "Sum rate maximization for MU-MISO with partial CSIT using joint multicasting and broadcasting," in *2015 IEEE International Conference on Communications (ICC)*, June 2015, pp. 4733–4738.
- [26] J. Xu, L. Qiu, and C. Yu, "Improving energy efficiency through multi-mode transmission in the downlink MIMO systems," *EURASIP Journal on Wireless Communications and Networking*, vol. 2011, no. 1, p. 200, 2011.
- [27] M. Grant, S. Boyd, and Y. Ye, "CVX: Matlab software for disciplined convex programming," 2008.
- [28] A. Wiesel, Y. C. Eldar, and S. Shamai, "Linear precoding via conic optimization for fixed mimo receivers," *IEEE Transactions on Signal Processing*, vol. 54, no. 1, pp. 161–176, Jan 2006.